Effect of Supplemental Viscous Damping on the Seismic Response of Structural Systems with Metallic Dampers

Ramiro Vargas[1] and Michel Bruneau[2]

Abstract: Metallic dampers can enhance structural performance by reducing seismically induced lateral displacements, and by reducing inelastic behavior of beams and columns. Limiting story drift also indirectly allows us to mitigate damage of nonstructural components that are sensitive to lateral deformations. However, many nonstructural elements and components are vulnerable to excessive accelerations. Therefore, in order to protect these components, floor accelerations in buildings should be kept below certain limits. In this perspective, this paper investigates the seismic performance of single-degree-of-freedom (SDOF) systems with metallic and viscous dampers installed in parallel, to determine the effectiveness or appropriateness of using metallic dampers to mitigate lateral displacements, simultaneously with viscous dampers to reduce acceleration demands, knowing that their behavior is fundamentally different (i.e., metallic dampers are displacement dependent, whereas velocity dampers are velocity dependent). The effect of a combination of these damping systems is, therefore, studied for SDOF structures as a contribution to the state-of-the-art of seismic protection of nonstructural components. Parametric analyses investigate the effectiveness of adding various levels of viscous damping on the equivalent hysteretic damping and on the spectral floor acceleration for short, intermediate, and long period structures. Argand diagrams are used to explain why in some instances it is observed that adding viscous dampers to strongly inelastic systems can result in increases in floor acceleration (rather than the intended decreases). Results from this study are also applicable to buildings that have been retrofitted with viscous dampers and whose original frame still behaves inelastically after the retrofit.

DOI: 10.1061/(ASCE)0733-9445(2007)133:10(1434)

CE Database subject headings: Damping; Seismic effects; Displacement; Beams; Columns; Inelasticity.

Introduction

In the 1964 Alaska and 1971 San Fernando earthquakes, extensive damage of nonstructural components was observed, which resulted in substantial economic losses, serious casualties, and impediments to the buildings operation, even in buildings that suffered limited or no structural damage (Lagorio 1990). Consequently, since the 1970s, many research projects have focused on providing guidance to design, retrofit, and improve the seismic performance of nonstructural elements. An inventory and summary of past research, as well as comparisons of existing regulations to seismically design nonstructural components, can be found in Filiatrault et al. (2002), where, as part of the study, recommendations are made for the development of a comprehensive research plan to investigate the seismic performance of nonstructural building components.

Metallic dampers (hysteretic dampers), especially designed to behave as passive energy dissipation (PED) devices, have been thoroughly studied in the past to enhance structural performance by reducing seismically induced structural damage. In this sense, metallic dampers have been implemented primarily in flexible framing systems (e.g., moment frames) to reduce interstory drifts, and eliminate (or at least reduce) inelastic behavior in beams and columns (Bruneau et al. 1998). Limiting story drift allows us to mitigate damage of nonstructural components that are sensitive to lateral deformations (i.e., elements that are generally attached to consecutive floors). However, many nonstructural elements and equipment are attached to a single floor, and can lose their functionality due to excessive sliding, overturning, or damage to their internal components due to severe floor vibrations. In order to protect these components, floor acceleration and, in some cases, floor velocity (e.g., in the case of toppling of furniture) should be kept under certain limits.

Although metallic dampers have been shown to be effective to reduce interstory drifts, some studies have found that, in many cases, the use of metallic dampers may cause increases in floor accelerations due to the added stiffness, which may negatively affect seismic behavior of nonstructural components (e.g., Iwata 2004; Mayes et al. 2004; Tong et al. 2003; to name a few). This suggests that it may be desirable to use metallic dampers to mitigate lateral displacements, along with viscous dampers to reduce acceleration demands. In this perspective, this paper investigates the seismic performance of single-degree-of-freedom (SDOF) systems with metallic and viscous dampers installed in parallel, knowing that their behavior is fundamentally different (i.e., metallic dampers are displacement dependent, whereas velocity dampers are velocity dependent). The effect of a combination of these damping systems is, therefore, studied for SDOF structures

[1]Assistant Professor, Dept. of Civil Engineering, Technological Univ. of Panama, PTY #12450, P.O. Box 25207, Miami, FL 33102 (corresponding author). E-mail: ramiro.vargas@utp.ac.pa

[2]Professor and MCEER Director, Dept. of Civil, Structural and Environmental Engineering, State Univ. of New York at Buffalo, 130 Ketter Hall, Buffalo, NY 14260. E-mail: bruneau@buffalo.edu

Note. Associate Editor: Michael D. Symans. Discussion open until March 1, 2008. Separate discussions must be submitted for individual papers. To extend the closing date by one month, a written request must be filed with the ASCE Managing Editor. The manuscript for this paper was submitted for review and possible publication on October 26, 2005; approved on February 27, 2007. This paper is part of the ***Journal of Structural Engineering***, Vol. 133, No. 10, October 1, 2007. ©ASCE, ISSN 0733-9445/2007/10-1434–1444/$25.00.

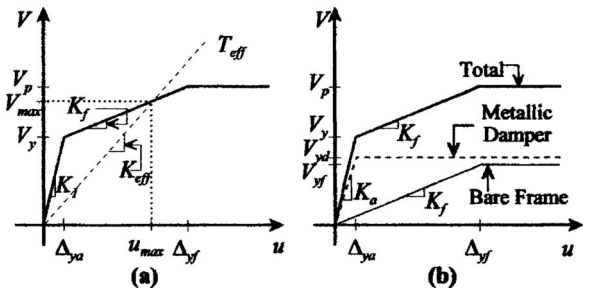

Fig. 1. General pushover curve: (a) effective stiffness and period; (b) bare frame and metallic damper contribution to total base shear capacity

as a contribution to the state-of-the-art of the seismic protection of nonstructural components.

Parametric analyses of hysteretic damping and spectral acceleration are presented for short, intermediate, and long period structures with different levels of viscous damping. Response in the frequency domain is also shown as graphics of inertial, viscous damper, and hysteretic forces represented in the complex plane. These results are used to provide a preliminary assessment of the effectiveness of using metallic and viscous dampers in parallel to reduce floor accelerations.

Viscous Damping

Viscous fluid dampers have been widely studied in the past, and significant efforts have been directed to implement these devices in structural systems (Soong and Dargush 1997). Viscous fluid dampers generally work on the principle of energy dissipation of incompressible fluids forced to flow through orifices (Constantinou and Symans 1992). The viscous damping force, F_d, is proportional to the velocity of motion, $\dot{u}$, according the following expression:

$$F_d = c|\dot{u}|^{\beta}\text{sgn}(\dot{u}) \tag{1}$$

where β takes values between 0.3 and 2.0; and c=damping coefficient. According to Hanson and Soong (2001), small values of β (i.e., $\beta \leq 0.5$) are effective to mitigate high-velocity shocks, such as isolation of military hardware. On the other hand, in applications of structural engineering, $\beta = 1$ is usual desirable to design systems against wind or earthquake loads (Hanson and Soong 2001), and therefore it is the value used in this study.

Equivalent Viscous Damping (Hysteretic Damping)

In many structural analyses such as the nonlinear static procedure FEMA (FEMA 2000), the dynamic characteristics of a structure having metallic dampers are transformed to an effective period, T_{eff}, which is obtained from the secant or effective stiffness, K_{eff}, of the combined system (i.e., bare frame plus dampers) to the point of maximum displacement as illustrated in Fig. 1(a), the inherent viscous damping, ξ_v, and an equivalent viscous damping (hysteretic damping) for the metallic dampers, ξ_h, also determined from specific hysteresis loops at the point of maximum displacement. Generally, the hysteretic damping for a metallic damper is obtained by setting the area within a hysteresis loop equal to the area within a viscous damper cycle, provided that the area contained within one cycle of motion is the energy dissipated per cycle (Hanson and Soong 2001).

Consequently, the hysteretic damping, ξ_h, may be determined from the following expression, adapted from Ramirez et al. (2001):

$$\xi_h = \frac{2q_h(1 - 1/\mu_f) + 2(V_{yd}/V_{yf})(1 - 1/\mu)}{\pi(1 + V_{yd}/V_{yf})} \geq 0 \tag{2}$$

where q_h=quality factor of the loop, taken as 1.0 for bilinear systems; V_{yf} and V_{yd}=contributions from the bare frame and from the metallic damper to the base shear capacity, respectively; μ and μ_f=global and frame ductility determined as $u_{\max}/\Delta_{ya}$ and $u_{\max}/\Delta_{yf}$, respectively [see Fig. 1(b)], where $u_{\max}$=system maximum lateral displacement; and Δ_{ya} and Δ_{yf}=yield displacement of the metallic dampers, and the yield displacement of the frame, respectively.

The set of parameters used in this study are obtained from Fig. 1(b): the strain-hardening ratio, α, the maximum displacement ductility, $\mu_{\max}$, and the strength ratio, η. The strain-hardening ratio, α=relation between the frame stiffness, K_f, and the total initial stiffness, K_1 which can be calculated as

$$\alpha = \frac{1}{1 + \dfrac{K_a}{K_f}} \tag{3}$$

where K_a=stiffness of the added damping system; and α=dimensionless parameter less than one. The maximum displacement ductility is the maximum displacement ductility that the structure experiences before the frame undergoes inelastic deformations. This parameter can be written as

$$\mu_{\max} = \frac{\Delta_{yf}}{\Delta_{ya}} \tag{4}$$

with $\mu_{\max}$ being greater than one. The strength ratio, η, is determined as the relation between the yield strength and the peak effective ground force applied during the motion, defined as

$$\eta = \frac{V_y}{m\ddot{u}_{g\max}} \tag{5}$$

where m=mass; V_y=yield strength of the system; and $\ddot{u}_{g\max}$=peak ground acceleration. Substituting $q_h = 1.0$; $V_{yd} = V_y(1-\alpha)$; and $V_{yf} = V_y \alpha \mu_{\max}$ [which can be determined from Fig. 1(b)] into Eq. (2), gives

$$\xi_h = \left(\frac{2}{\pi}\right)\left[\frac{(1 - 1/\mu_f) + \dfrac{(1-\alpha)}{\alpha\mu_{\max}}(1 - 1/\mu)}{1 + \dfrac{(1-\alpha)}{\alpha\mu_{\max}}}\right] \geq 0 \tag{6}$$

which expression used in this study. Note that for $\mu < 0$ (and therefore, $\mu_f < 0$), the system remains elastic, which translates into no dissipation of energy through hysteretic behavior and, therefore, no hysteretic damping is developed (i.e., $\xi_h = 0$).

Parametric Analysis of Hysteretic Damping

A parametric study was conducted to analyze how the hysteretic damping, ξ_h, is affected by increasing the viscous damping, $\Delta\xi_v$, in SDOF systems with metallic dampers. A design response spectrum was constructed based on the National Earthquake Hazard

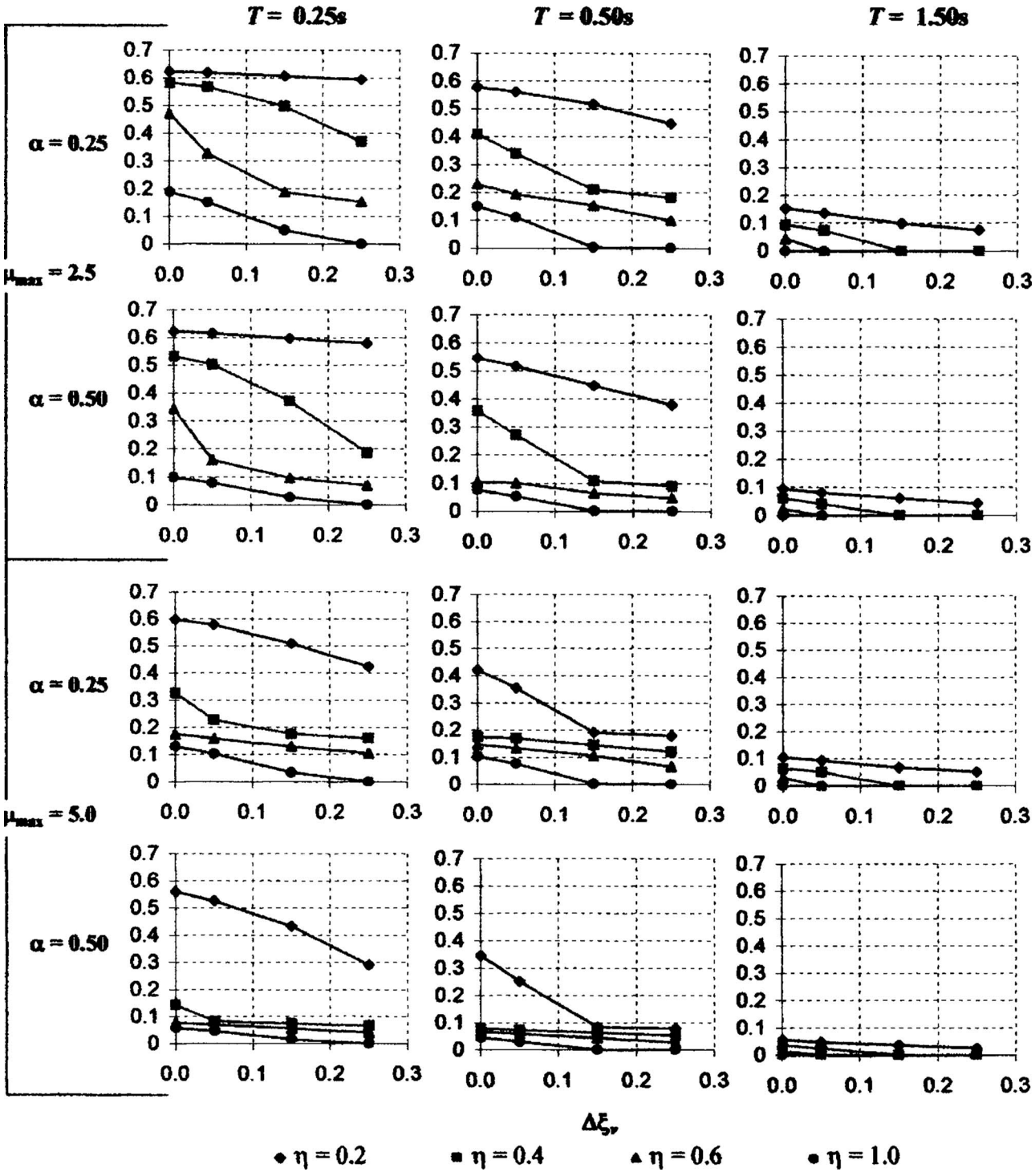

Fig. 2. Hysteretic damping, ξ_h, versus increase in viscous damping, $\Delta\xi_v$

Reduction Program Recommended Provisions FEMA 450 (FEMA 2003) for Sherman Oaks, Calif., and site soil-type class B. This site was chosen because it corresponds to the location of a demonstration hospital used by the Multidisciplinary Center for Earthquake Engineering Research (MCEER) in some of its projects. Accordingly, the design spectral accelerations for this site are $S_{DS}=1.3\ g$, and $S_{Dl}=0.58\ g$. Using the target acceleration spectra compatible time histories (TARSCTHS) code, by Papageorgiou et al. (1999), three spectra-compatible synthetic ground motions were generated to match the FEMA 450 target design spectrum. Nonlinear time history analyses were conducted using the Structural Analysis Program (SAP) 2000 (Computers and Structures Inc. 2000). Analyses were performed for the following parameters: $\alpha=0.25$, 0.50; $\mu_{max}=2.5$, 5.0; and $\eta=0.2$, 0.4, 0.6, 1.0. Analyses were also conducted for values of $\alpha=0.05$ and $\mu_{max}=1.67$, 10 (Vargas and Bruneau 2006), but these other cases are not included here due to space constraints. Short, intermediate, and long period structures ($T=0.25$, 0.50, and 1.50 s, respectively) were then analyzed for increases in viscous damping, $\Delta\xi_v$, of 0, 5, 15, and 25% from a base value of 5%. Hysteretic damping

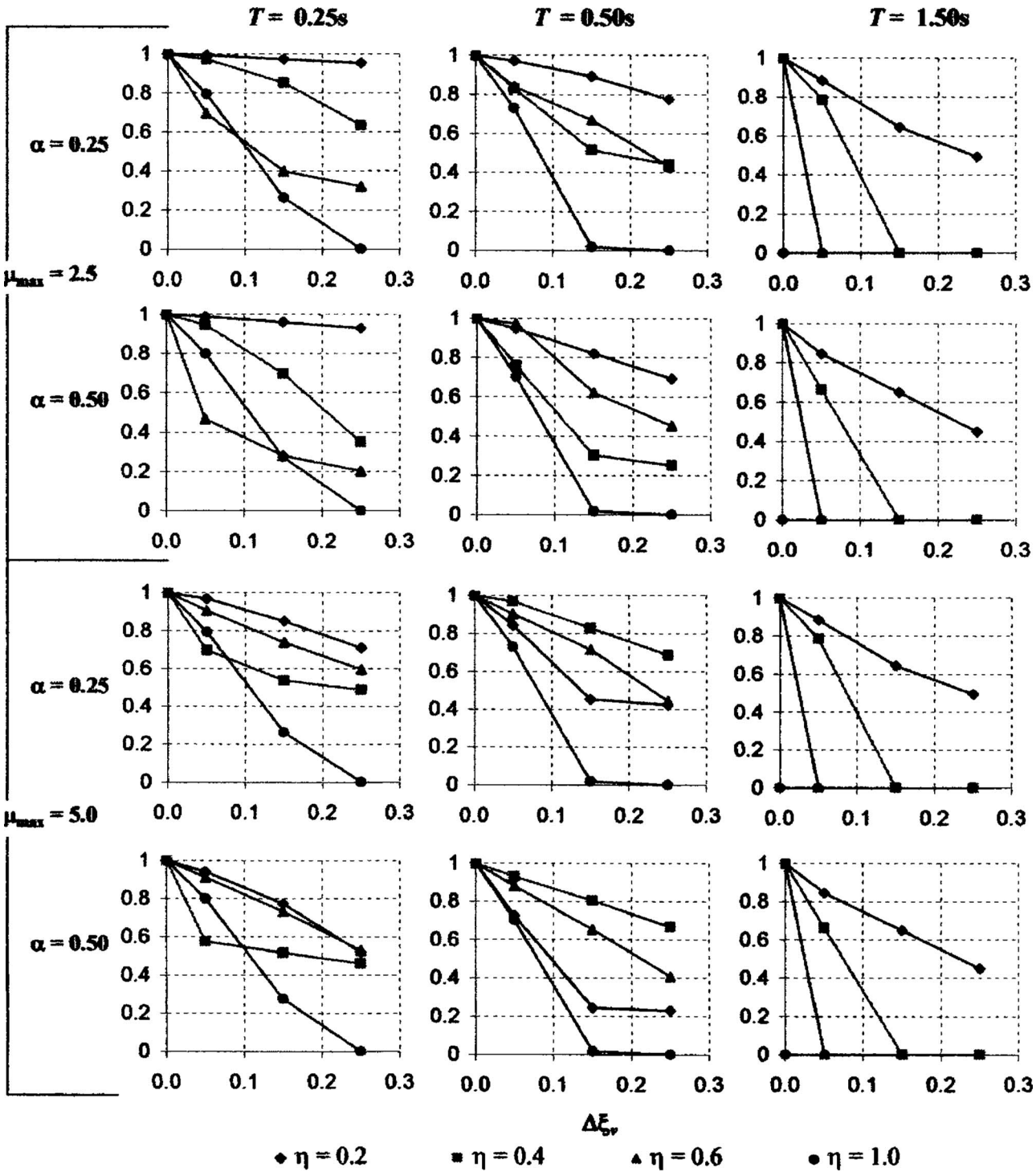

Fig. 3. Ratio of hysteretic damping with respect to original hysteretic damping, ξ_h/ξ_{h0}, versus increase in viscous damping, $\Delta\xi_v$

was determined using Eq. (6), for a given set of parameters, and the values of global ductility, μ, and frame ductility, μ_f, obtained from the system response.

Fig. 2 shows how the hysteretic damping, ξ_h, decreases with increases in viscous damping, $\Delta\xi_v$, for system periods of 0.25, 0.50, and 1.50 s, respectively. This is because the hysteretic damping is proportional to the ductility demand, which decreases with increases in viscous damping [see Eq. (6)]. Since hysteretic damping is proportional to ductility demand, all the observed relationships between ductility demand and key parameters (i.e., α, μ_{max}, η, and T) can help to explain how hysteretic damping relates to the same key parameters. For instance, in Vargas and Bruneau (2006) it was found that increases in both α and μ_{max} result in decreases in the ductility demand for systems without viscous dampers (shown in Fig. 2 at $\Delta\xi_v=0$), which lead to a significant reduction in the hysteretic damping. Vargas and Bruneau (2006) also observed that the ductility demand reduces with increases in η and T, which again result in decreases in the hysteretic damping. Note that the largest values of hysteretic damping were obtained for systems having small values of α, μ_{max}, η, and T; whereas, the smallest values of hysteretic damping were obtained for large values of these parameters. For

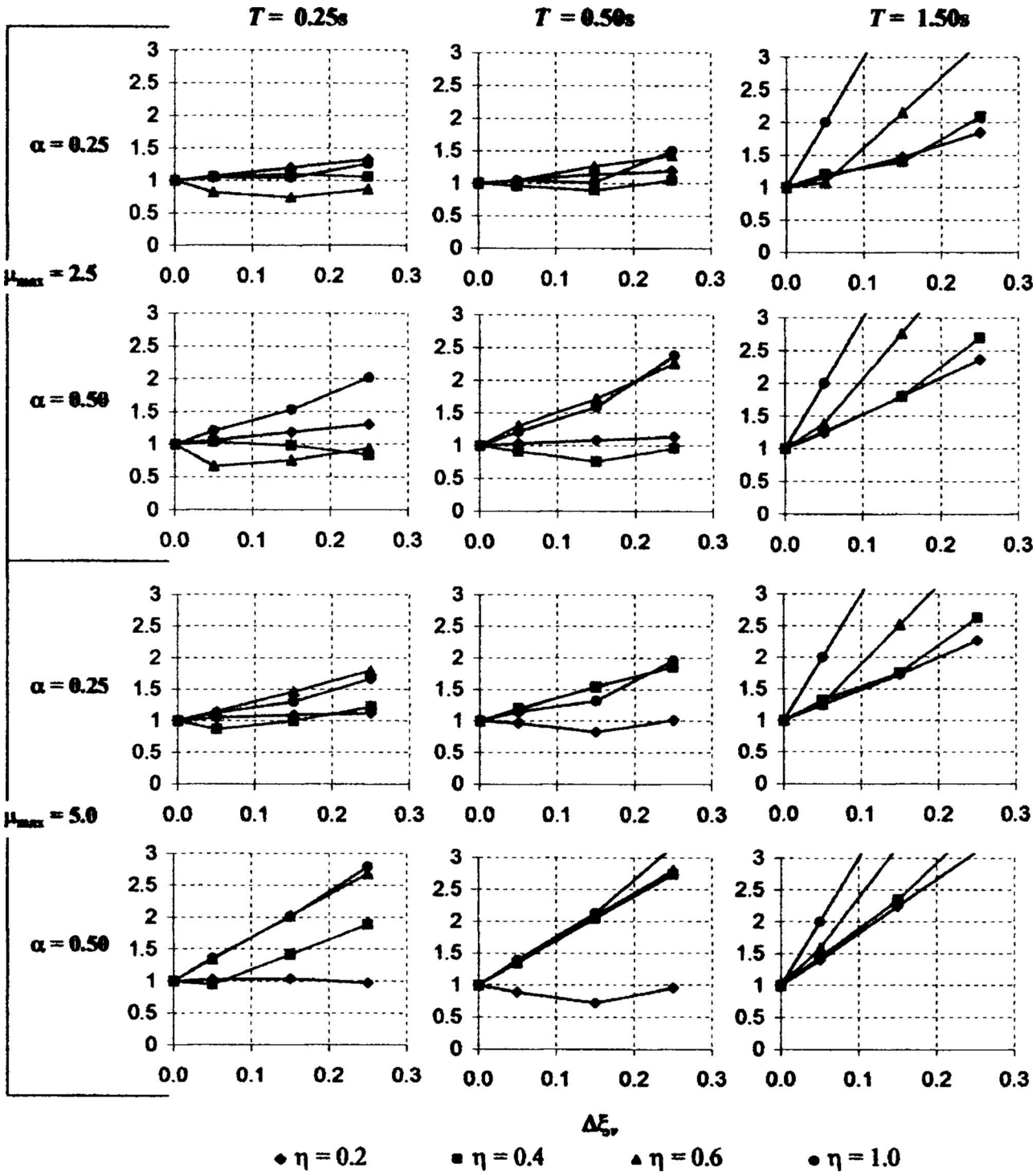

Fig. 4. Ratio of total damping with respect to original damping, ξ_t/ξ_{t0}, versus increase in viscous damping, $\Delta\xi_v$

example, in a short period system (T=0.25 s) with α=0.25, μ_{max}=2.5, and η=0.4, the hysteretic damping reduces from 58 to 37% when viscous damping is increased by 25%. On the other hand, in a long period system (T=1.50 s) with α=0.50, μ_{max}=5, and η=0.6, the hysteretic damping reduces from 1 to 0% when viscous damping is increased by 5%, as the system becomes elastic and remains elastic even if viscous damping is further increased.

In Fig. 3, the ratio of the hysteretic damping with respect to the hysteretic damping of the original system, ξ_h/ξ_{h0}, is plotted versus the increase in viscous damping, $\Delta\xi_v$. In this study, a reference system with viscous damping of 5%, along with its corresponding hysteretic damping, ξ_{h0}, is called the "original system." Fig. 3 show how "fast" the hysteretic damping is reduced by increases in the viscous damping due to decreases in the ductility demand [Eq. (6)]. Note that in long period systems the hysteretic damping reduces "faster" to the level of elastic response (i.e., ξ_h=0) than in short period structures. This is because the ductility demand has smaller values for long period original systems, and

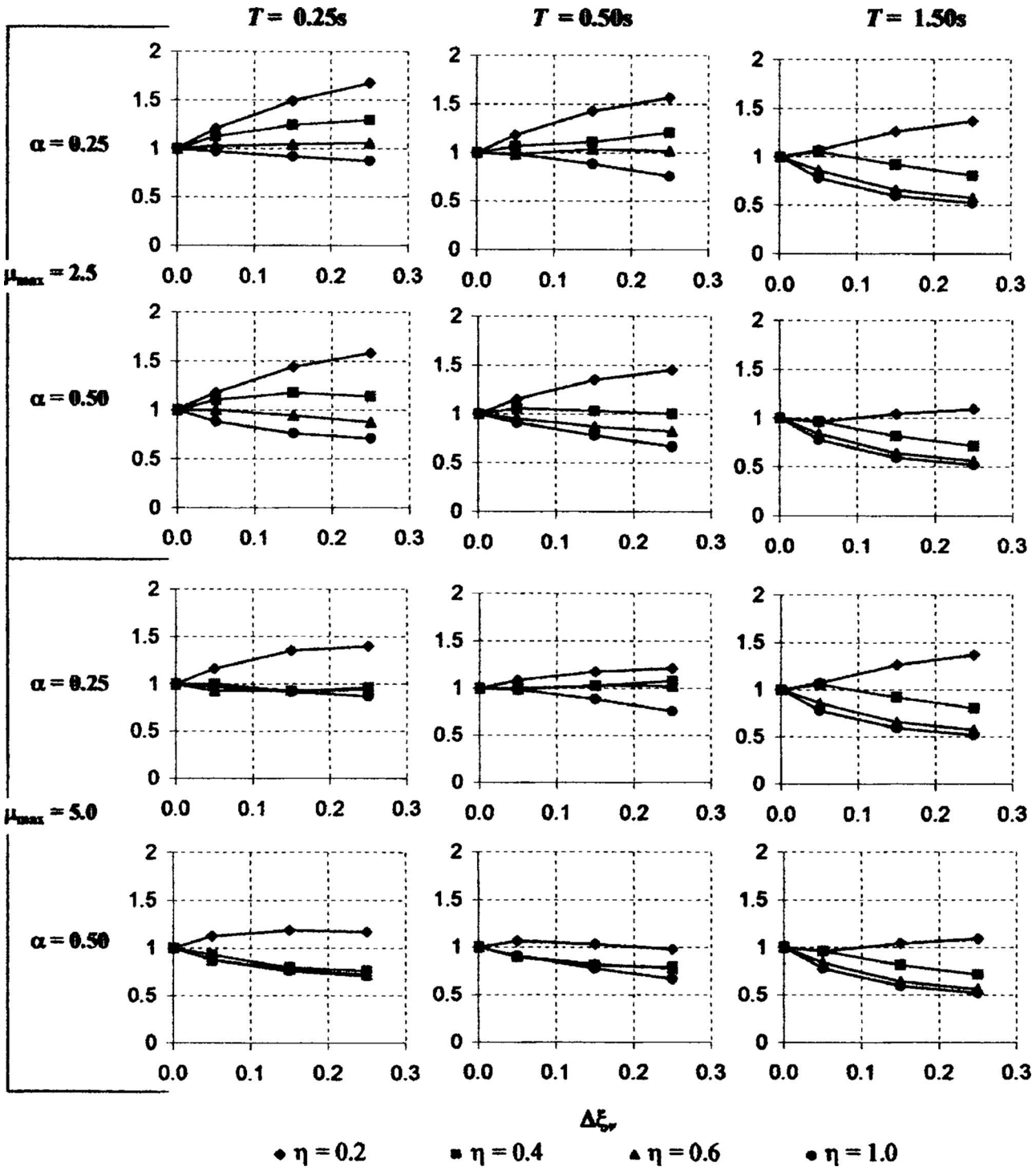

Fig. 5. Ratio of floor spectral acceleration with respect to original floor spectral acceleration, S_a/S_{a0}, versus increase in viscous damping, $\Delta\xi_v$

therefore, small increases in viscous damping can make the structure respond elastically (see Fig. 2).

Furthermore, in Fig. 4 the ratio of total damping with respect the total damping of the original system, ξ_t/ξ_{to}, is plotted versus the increase in viscous damping, $\Delta\xi_v$. Total damping is determined summing the contributions from viscous and hysteretic damping, using the following expressions

$$\xi_{to} = \xi_{v0} + \xi_{h0} = 0.05 + \xi_{h0} \tag{7}$$

$$\xi_t = \xi_v + \xi_h = 0.05 + \Delta\xi_v + \xi_h \tag{8}$$

Because hysteretic damping decreases nonlinearly with increases in viscous damping, the total damping, ξ_t, calculated using Eq. (8), may result in a gain or loss of equivalent damping, depending on the relative values of $\Delta\xi_h$ and $\Delta\xi_v$. In Fig. 4, a value of $\xi_t/\xi_{to} > 1.0$ corresponds to a gain of total damping (i.e., $\Delta\xi_v > |\Delta\xi_h|$). Note also that for short and intermediate period systems having $\alpha = 0.25$ and $\mu_{max} = 2.5$, increases in viscous

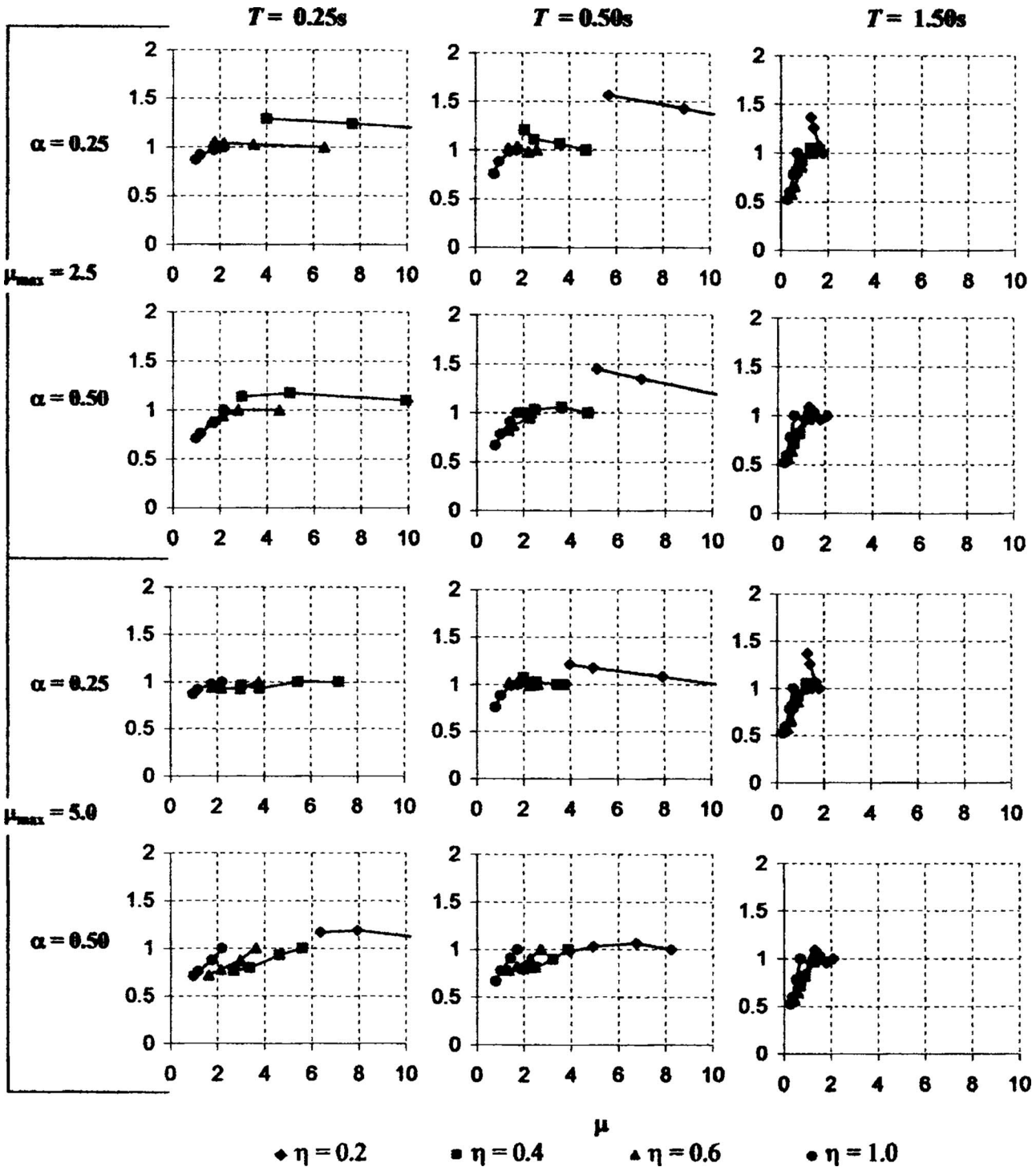

Fig. 6. Ratio of spectral acceleration with respect to original floor spectral acceleration, S_a/S_{a0}, versus global ductility, μ

damping tend to be compensated for by decreases in hysteretic damping (i.e., $\Delta\xi_v \approx |\Delta\xi_h|$), and therefore, no significant gain of total damping is appreciated. On the other hand, in long period structures, significant gains of total damping are consistently observed (i.e., $\Delta\xi_v \gg |\Delta\xi_h|$), since elastic behavior of the system is "quickly" achieved by increases in viscous damping (i.e., $\xi_h=0$). For example, in a short period system ($T=0.25$ s) with $\alpha=0.25$, $\mu_{max}=2.5$, and $\eta=0.4$, the total damping increases by a factor of 1.06 when viscous damping is increased by 25%. On the other hand, in a long period system ($T=1.50$ s) with $\alpha=0.50$, $\mu_{max}=5$, and $\eta=0.6$, the total damping increases by a factor of 4.76 when viscous damping is increased by 25%.

Parametric Analysis of Spectral Acceleration

A parametric study was conducted to analyze how floor accelerations are affected by increases in viscous damping in SDOF systems with metallic dampers, using the set of synthetic earthquakes and parameters established for this study.

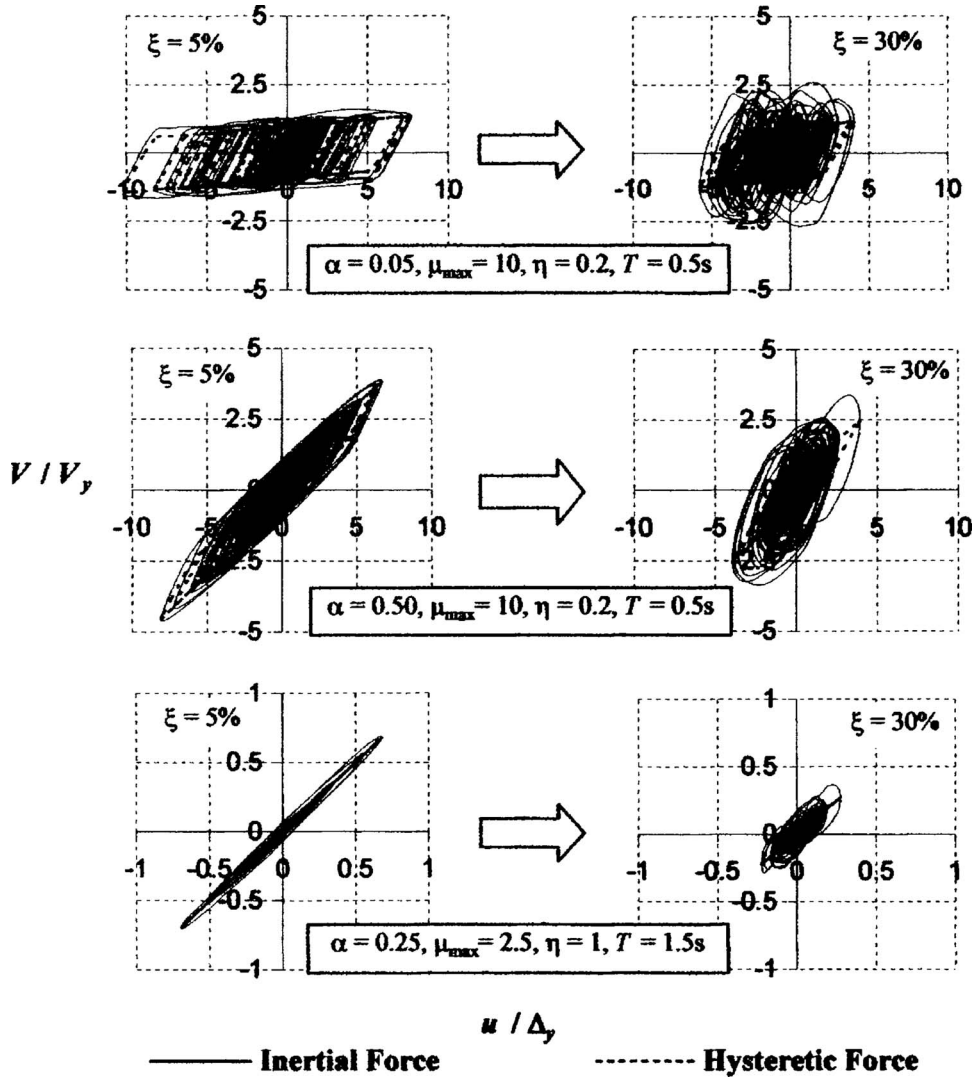

Fig. 7. Normalized inertial and hysteretic loops for 5 and 30% of viscous damping

In Fig. 5, response was plotted as a ratio of floor spectral acceleration, S_a, with respect to the floor spectral acceleration of the original system, S_{a0}, for systems with periods of 0.25, 0.50, and 1.50 s, respectively. It may be noted that for short and intermediate period systems, the spectral acceleration increases with viscous damping, except for large values of α and μ_{max} (i.e., $\alpha=0.5$ and $\mu_{max}=5$) where a reduction in spectral acceleration may be seen for values of $\eta \geqslant 0.4$. For example, in a short period system ($T=0.25$ s) with $\alpha=0.25$, $\mu_{max}=2.5$, and $\eta=0.4$, the spectral acceleration increases by a factor of 1.29 when viscous damping is increased by 25%. However, in a short period system ($T=0.25$ s) with $\alpha=0.50$, $\mu_{max}=5$, and $\eta=0.6$, the spectral acceleration is reduced by 28% when viscous damping is increased by 25%.

On the other hand, for long period structures, the spectral acceleration generally decreases with increases in the viscous damping, except for small η values (i.e., $\eta=0.2$). These results agree with the fact that, for long period systems, the total damping substantially increases with viscous damping, since the reduction in hysteretic damping is insignificant (i.e., $\Delta\xi_h \approx 0$, and $\Delta\xi_v \gg |\Delta\xi_h|$). For example, in a long period system ($T=1.50$ s) with $\alpha=0.25$, $\mu_{max}=2.5$, and $\eta=0.4$, the spectral acceleration reduces by 19% when viscous damping is increased by 25%. However, in a long period system ($T=1.50$ s) with $\alpha=0.50$, $\mu_{max}=5$, and $\eta=0.2$, the spectral acceleration slightly increases by 9% when viscous damping is increased by 25%.

Fig. 6 shows the relationship between S_a/S_{a0} and global ductility, μ, recalling that both are affected by increases in viscous damping (i.e., the highest value of μ in every curve corresponds to $\Delta\xi_v=0$, and the lowest one corresponds to $\Delta\xi_v=25\%$). Note that original systems that respond with a ductility approximately equal to two (i.e., $\mu \approx 2$ for $\Delta\xi_v=0$), are more likely to have a reduction in acceleration demands by increases in viscous damping. This is because systems that have small ductility demands can be changed into systems that behave elastically by adding more viscous damping. In other words, adding viscous damping is effective in reducing accelerations and displacements response of systems that behave elastically, or that can be modified such as to behave elastically (Chopra 2001). For example, in a long period system ($T=1.50$ s) with $\alpha=0.50$, $\mu_{max}=5$, and $\eta=0.4$, the global ductility, μ, reduces from 1.51 to 0.68, and the spectral acceleration is reduced by 29% when viscous damping is increased by 25%. Subsequent sections are devoted to further investigate the relationship between viscous damping and acceleration response of elastic and inelastic systems.

Hysteretic Response

As previously mentioned, the main purpose of this paper is to investigate whether using viscous fluid dampers in parallel with metallic dampers can simultaneously reduce lateral displacements and floor accelerations. Although lateral displacement always decreases when using metallic, viscous, or both kind of dampers acting together, it was found (in the previous section) that floor acceleration increases in most of the cases considered, even for systems designed with large viscous damping. This section focuses on studying the hysteretic response of short, intermediate, and long period systems, using the lowest and highest values of η from previous analyses (i.e., $\eta=0.2$ and $\eta=1.0$), along with several levels of viscous damping (i.e., 5, 10, 20, and 30%), to understand the reason for these observed increases in acceleration.

Using d'Alembert's principle, it is possible to express the equation of motion of a SDOF system as an equation of dynamic equilibrium (Clough and Penzien 1993). Therefore, for a SDOF subjected to ground excitation, the equation of motion may be written as

$$F_i + F_d + F_s = 0 \tag{9}$$

where F_i is the inertial force, calculated as

$$F_i = \boldsymbol{m}(\ddot{u}_g + \ddot{u}) \tag{10}$$

where $\ddot{u}_g$ and $\ddot{u}$=ground acceleration, and the relative floor acceleration, respectively; F_d=viscous damper force calculated using Eq. (1); and F_s=sum of the metallic damper force and the structural frame force, called here the hysteretic force, determined according to the following expression

$$\begin{aligned} &F_s = K_1 u, && u < \Delta_{ya} \\ &F_s = V_y + \alpha K_1 (u - \Delta_{ya}), && \Delta_{ya} \leq u < \Delta_{yf} \\ &F_s = V_p, && \Delta_{yf} \leq u \end{aligned} \tag{11}$$

where all variables are defined in Fig. 1. Note that for undamped systems (i.e., $F_d=0$), the inertial and hysteretic forces must be equal and opposite to satisfy the dynamic equilibrium of Eq. (9). In damped systems, increases in viscous damping (i.e., increases in the damping ratio) result in decreases in the lateral displacement, u, and therefore, decreases in the hysteretic force, F_s, according to Eq. (11) (assuming that the system is designed such that $u<\Delta_{yf}$, which is required to prevent any inelastic behavior of the frame). Consequently, acceleration demand, $\ddot{u}$, may increase (or decrease) to satisfy dynamic equilibrium. The resultant increase or decrease in the inertial force depends on the increase in the F_d value relative to the decrease in the value of F_s. For instance, if $\Delta F_d > |\Delta F_s|$ then $\Delta\ddot{u}>0$ (i.e., acceleration increases), and if $\Delta F_d < |\Delta F_s|$ then $\Delta\ddot{u}<0$ (i.e., acceleration decreases).

Fig. 7 shows some examples of the superposed hysteresis loops for the inertial force and hysteretic force normalized with respect to the yield point (V_y, Δ_{ya}). The difference between the curves is equal to the viscous damper force, F_d. Note that when the maximum displacement is reached (i.e., $\dot{\boldsymbol{u}}=\boldsymbol{0}$) the values of both curves coincide (i.e., $|F_i|=|F_s|$). The maximum difference between the curves is obtained when $u=0$, since the hysteretic force has its minimum value at this point. For elastic systems (i.e., $u<\Delta_{ya}$), when $u=0, F_s=0$, the inertial force and the damping force are equal (i.e., $|F_i|=|F_d|$).

Note that for systems that behave inelastically and for which the frame remains elastic (i.e., $\Delta_{ya}\leq u<\Delta_{yf}$), the strain-hardening ratio, α, has a significant influence on the acceleration demand, since $F_s=V_y+\alpha K_1(u-\Delta_{ya})$ in this region. Since $F_s \approx V_y$ in systems with small values of α, a reduction in the hysteretic force when viscous damping is added is not significant. On the other hand, F_s may be significantly reduced in systems with large values of α, when maximum displacement decreases by the addition of viscous damping. For example, in a system with $T=0.5$ s, $\eta=0.2$, $\alpha=0.05$, $\mu_{max}=10$ (Fig. 7), the hysteretic force remains almost constant (i.e., $\Delta F_s \approx 0$), and the acceleration demand consequently increases by about 60%, when 25% of extra viscous damping is added. For the same system, but with $\alpha=0.50$ instead, F_s is reduced by 40% when 25% of viscous damping is added (i.e., $\Delta F_d < |\Delta F_s|$), and accordingly, the acceleration demand decreases by about 30%.

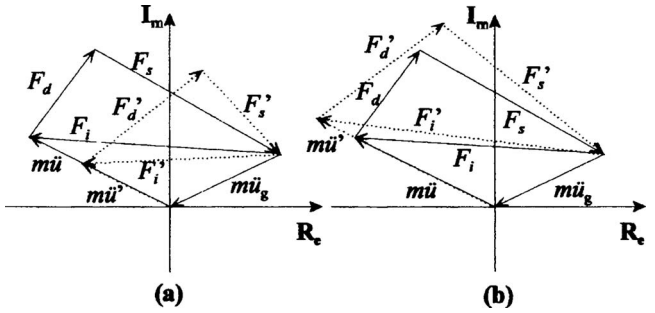

Fig. 8. Schematic representation of inertial, viscous damper and metallic damper forces: (a) elastic systems; (b) inelastic systems

Also, it may be noted in Fig. 7 that for elastic systems (i.e., $F_s=K_1u$), the displacement and acceleration demands both decrease by increasing the viscous damping, since the decrease in the hysteretic force is always larger than the increase in the viscous damper force (i.e., $\Delta F_d < |F_s|$). For example, in a system with $T=1.50$ s, $\eta=1.0$, $\alpha=0.25$, $\mu_{max}=2.5$, the hysteretic force reduces by 40% when 25% of viscous damping is added (i.e., $\Delta F_d < |\Delta F_s|$), and the acceleration demand accordingly decreases by about 50%.

These results corroborate the fact that the addition of viscous damping is effective in reducing the displacements and acceleration demands of elastic or near-elastic (e.g., $\alpha=0.5$) systems, but is less effective for nonlinear systems. However, metallic dampers with elastic behavior are not effective, since they only provide additional stiffness to reduce lateral displacements, which is something that could be done just as well with conventional structural elements (Vargas and Bruneau 2006).

Analysis in Frequency Domain

Results from the systems previously studied are analyzed in this section in the frequency domain. Using the fast Fourier transform (FFT) algorithm (Cooley and Tukey 1965), response of the systems studied parametrically here were transformed from the time domain to the frequency domain, in which inertial, viscous damper, and hysteretic forces can be represented as rotational vectors forming a closed polygon in the complex plane, as schematically shown in Fig. 8 (also called Argand diagrams) (Clough and Penzien 1993). Fig. 8(a) shows a representation of the equation of motion [Eq. (9)] for a system with elastic behavior at a particular time during the earthquake time history. Note that increases in the viscous damper force result in substantial decreases in the hysteretic and in the inertial forces (shown as dotted lines). On the other hand, in systems with inelastic behavior [Fig. 8(b)] an increase in the viscous damper force may result in a substantial

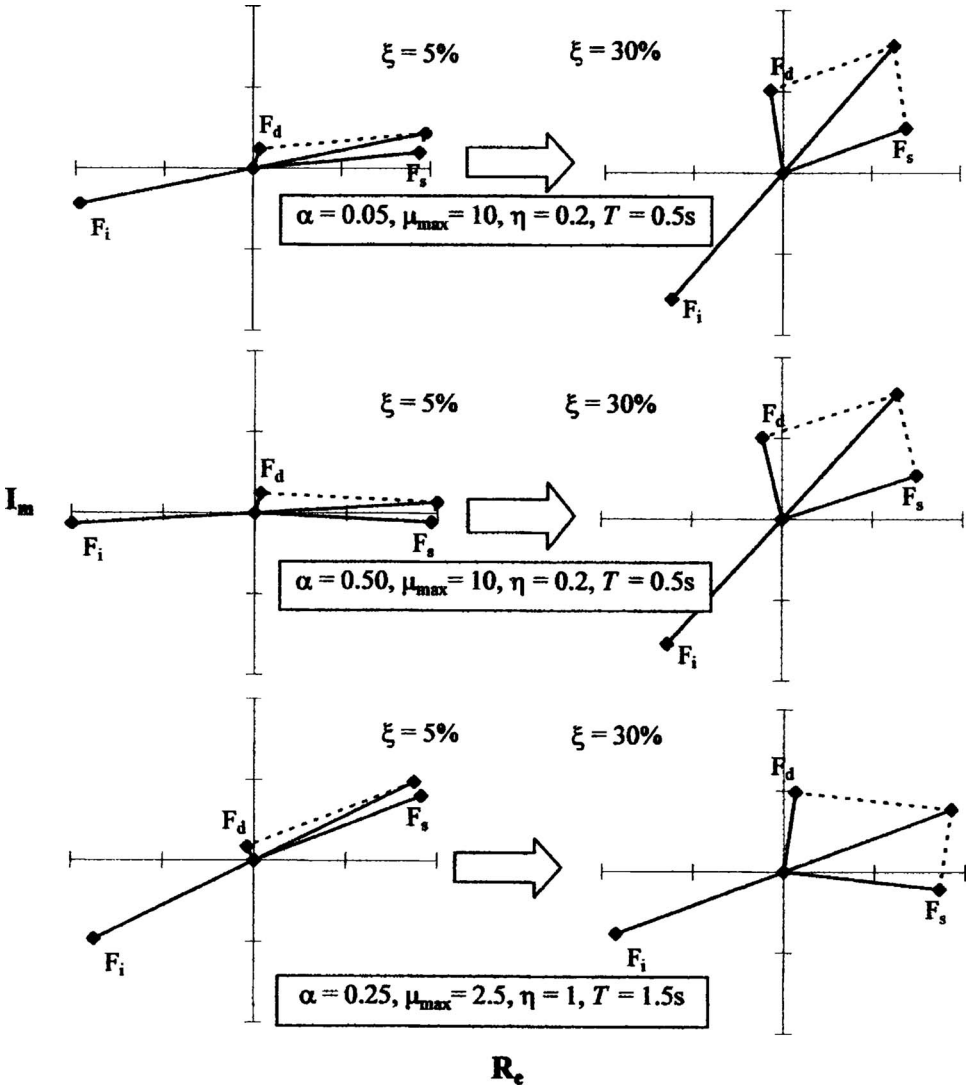

Fig. 9. Complex plane representation of inertial force, F_i, viscous damper force, F_d, and metallic damper force, F_s, for 5 and 30% of viscous damping

increase in the inertial force along with a slight decrease in the hysteretic force (shown again as dotted lines).

Response of the systems presented in Fig. 7 was transformed to the frequency domain and shown in Fig. 9. Every plot corresponds to the maximum value of inertial force obtained during the time history of response, along with the corresponding viscous and hysteretic forces at that particular time. All the forces are normalized with respect to the inertial force (i.e., inertial force is plotted as an unitary vector, and viscous and hysteretic forces are represented as fractions of the inertial force). From Eq. (9) it may be noted that the resultant of the hysteretic and damping forces is equal and opposite to the inertial force, as is also shown in Fig. 9.

Note that for small viscous damping (i.e., 5%), the inertial force and the hysteretic force are almost equal. On the other hand, for systems with large viscous damping (i.e., 30%), the inertial force is considerably greater than the hysteretic force. This vectorial addition shows how a greater damping force can lead to the acceleration increases described in the previous section. Incidentally, this observation has been reported by some practitioners that have considered using viscous dampers to retrofit buildings in selective case studies, and have noticed increases in the floor accelerations if the structure remains inelastic after the retrofit but could not explain why (e.g., personal communication, Dr. Chris Tokas, Manager, California Hospital Seismic Retrofit Program, State of California Office of Statewide Health Planning and Development).

Conclusions

Seismic response of hybrid systems having metallic and viscous dampers has been studied in this paper through parametric analyses. It was found that increases in viscous damping reduce the effectiveness of metallic dampers in terms of energy dissipation, since the amplitude of motion (and thus ductility demand) is reduced. In some cases, when the amplitude of motion decreases to the point where the system behave elastically, metallic dampers only work to provide additional stiffness to the system, which may be achieved by other conventional methods (e.g., steel braces as opposed to special ductile devices).

Although viscous dampers are known to decrease both displacements and acceleration demands in structures with elastic behavior, for structural systems where metallic dampers are de-

signed to behave inelastically (i.e., $\Delta_{ya} \leqslant u < \Delta_{yf}$), the floor accelerations are likely to increase if viscous dampers are added in parallel to metallic dampers, especially for systems with small strain-hardening ratio (i.e., $\alpha < 0.25$). Therefore, adding such viscous dampers in parallel with hysteretic dampers could, in some instances, worsen the seismic performance of acceleration sensitive equipment and nonstructural components. This observation would also be true for buildings that have been retrofitted with viscous dampers and whose original frame still behaves inelastically under major earthquakes. Argand diagrams in the frequency domain are successfully used to explain these observations.

References

Bruneau, M., Uang, C. M., and Whittaker, A. (1998). *Ductile design of steel structures*, McGraw-Hill, New York.

Chopra, A. K. (2001). *Dynamics of structures*, 2nd Ed., Prentice-Hall, Upper Saddle River, N.J.

Clough, R. W., and Penzien, J. (1993). *Dynamics of structures*, 2nd Ed., McGraw-Hill, New York.

Computers and Structures Inc. (2000). *Structural analysis program, SAP-2000NL, version 8.3.5: Integral finite element analysis and design of structures*, Berkeley, Calif.

Constantinou, M. C., and Symans, M. D. (1992). "Experimental and analytical investigation of seismic response of structures with supplemental fluid viscous dampers." *Rep. No. NCEER-92-0032*, National Center for Earthquake Engineering Research, Univ. at Buffalo, State Univ. of New York, Buffalo, N.Y.

Cooley, J. W., and Tukey, J. W. (1965). "An algorithm for machine calculation of complex Fourier series." *Math. Comput.*, 9(90), 297–301.

Federal Emergency Management Agency. (2000). "Prestandard and commentary for the seismic rehabilitation of buildings." *Rep. No. FEMA 356*, Washington, D.C.

Federal Emergency Management Agency. (2003). "NEHRP recommended provisions for seismic regulations for new buildings and other structures." *Rep. No. FEMA 450*, Washington, D.C.

Filiatrault, A., Christopoulos, C., and Stearns, C. (2002). "Guidelines, specifications, and seismic performance characterization of nonstructural building components and equipment." *Rep. No. PEER-2002/05*, Pacific Earthquake Engineering Research Center, Univ. of California, Berkeley, Calif.

Hanson, R. D., and Soong, T. T. (2001). "Seismic design with supplemental energy dissipation devices." *Monograph No. MNO-8*, Earthquake Engineering Research Institute, Oakland, Calif.

Iwata, M. (2004). "Applications-design of buckling restrained braces in Japan." *Proc., 13th World Conf. on Earthquake Engineering*, Vancouver, Canada, Paper No. 3208.

Lagorio, H. J. (1990). *Earthquakes: An architect's guide to nonstructural seismic hazards*, Wiley, New York.

Mayes, R., Goings, C., Naguib, W., Harris, S., Lovejoy, J., Fanucci, J., Bystricky, P., and Hayes, J. (2004). "Comparative performance of buckling-restrained braces and moment frames." *Proc., 13th World Conf. on Earthquake Engineering*, Vancouver, Canada, Paper No. 2287.

Papageorgiou, A., Halldorsson, B., and Dong, G. (1999). "Target acceleration spectra compatible time histories." *TARSCTHS—User's manual*, version 1.0, Engineering Seismology Laboratory, State Univ. of New York, Buffalo, N.Y.

Ramirez, O. M., Constantinou, M. C. Kircher, C. A., Whittaker, A. S., Johnson, M. W., Gomez, J. D., and Chrysostomou, C. Z. (2001). "Development and evaluation of simplified procedures for analysis and design of buildings with passive energy dissipation systems." *Rep. No. MCEER-00-0010*, *Revision 1*, Multidisciplinary Center for Earthquake Engineering Research, Univ. at Buffalo, State Univ. of New York, Buffalo, N.Y.

Soong, T. T., and Dargush, G. F. (1997). *Passive energy dissipation systems in structural engineering*, Wiley, New York.

Tong, M., Lee, G. C., Rzhevsky, V., Qi, J., Shinozuka, M., and Middleton, J. (2003). "A comparison of seismic risk of nonstructural systems in a hospital before and after a major structural retrofit." *Proc., ATC-29-2 Seminar on Seismic Design, Retrofit, and Performance of Nonstructural Components in Critical Facilities*, Newport Beach, Calif.

Vargas, R., and Bruneau, M. (2006). "Analytical investigation of the structural fuse concept." *Rep. No. MCEER-06-004*, Multidisciplinary Center for Earthquake Engineering Research, State Univ. of New York at Buffalo, Buffalo, N.Y.